

A Reversible Crystallinity-Preserving Phase Transition in Metal–Organic Frameworks: Discovery, Mechanistic Studies, and Potential Applications

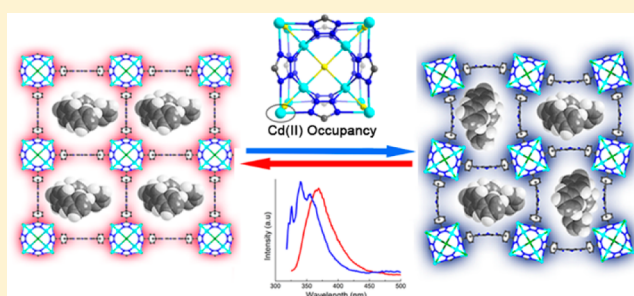
Dahuan Liu,^{†,‡,§} Tian-Fu Liu,^{†,§} Ying-Pin Chen,[†] Lanfang Zou,[†] Dawei Feng,[†] Kecheng Wang,[†] Qiang Zhang,[†] Shuai Yuan,[†] Chongli Zhong,[‡] and Hong-Cai Zhou^{*,†}

[†]Department of Chemistry, Texas A&M University, College Station, Texas 77842-3012, United States

[‡]State Key Laboratory of Organic-Inorganic Composites, Beijing University of Chemical Technology, Beijing 100029, China

S Supporting Information

ABSTRACT: A quenching-triggered reversible single-crystal-to-single-crystal (SC-SC) phase transition was discovered in a metal–organic framework (MOF) PCN-526. During the phase transition, the one-dimensional channel of PCN-526 distorts from square to rectangular in shape while maintaining single crystallinity. Although SC-SC transformations have been frequently observed in MOFs, most reports have focused on describing the resulting structural alterations without shedding light on the mechanism for the transformation. Interestingly, modifying the occupancy or species of metal ions in the extra-framework sites, which provides mechanistic insight into the causes for the transformation, can forbid this phase transition. Moreover, as a host scaffold, PCN-526 presents a platform for modulation of the photoluminescence properties by encapsulation of luminescent guest molecules. Through judicious choice of these guest molecules, responsive luminescence caused by SC-SC transformations can be detected, introducing a new strategy for the design of novel luminescent MOF materials.



INTRODUCTION

Single-crystal-to-single-crystal (SC-SC) phase transition has recently attracted great attention in the area of metal–organic frameworks (MOFs).^{1–6} Since MOFs maintain their single crystallinity throughout the transformation process, the change in structure can be precisely and straightforwardly characterized by single-crystal X-ray diffraction. This makes SC-SC phase transition an excellent opportunity to study the structure–property relationships of these functional materials in addition to methods of synthesizing them through rational design rather than trial and error. Generally, phase transition can be caused by chemical changes in the material, including the change of species (guest molecules/counterions/coordinated metal ions),² host–guest interactions,³ bond rearrangement, and topochemical reactions.⁴ In addition, phase transition can also be triggered by some physical stimuli, such as light, temperature, and pressure.^{5,6} Although SC-SC transformations have been observed in MOFs many times, most reports have focused on describing the resulting structural alterations without proposing mechanism or structural causes for the transformation. Obtaining precise structural information accounting for the phase transition is still an elusive goal, and the related research is very rare.^{2j} Moreover, there are few studies of potential applications employing the structural transformation. If the SC-SC transformation triggered by external stimuli can induce the change of another physical property of the material,

it would establish a responsive communication between these two properties. The technique to detect or indicate a complicated physical or chemical process by a readily detectable secondary responsive variable is very useful in many areas, such as industry and medicine.⁷ Herein, we report the synthesis of a MOF, PCN-526 (PCN: porous coordination network), based on tetrazolate porphyrinic ligands and cadmium clusters. PCN-526 exhibits a SC-SC transformation by an abrupt drop in temperature: the one-dimensional channel distorts from square to rectangular in shape when being cooled down from room temperature to 110 K and vice versa. Some efforts were then made to understand the mechanism of the phase transition. Interestingly, our investigation shows that the transformation can be forbidden by treating the crystals with solutions that can change the occupancy or species of the partially occupied metal ions in the extra-framework sites (around the metal cluster). These observations are testaments to the decisive role of the partially occupied metal ions, which may cause the phase transition by anisotropic stress or strain upon fast cooling. Furthermore, we were aiming to explore a physical property granted by the phase transition which may be taken advantage of for potential applications. Photoluminescence (PL) came to mind based on the fact that the energy transfer between two

Received: March 23, 2015

Published: May 26, 2015

photoactive molecules is usually very sensitive to the distance of chromophores. PL studies of pristine PCN-526 indicate that the SC-SC transformation did not result in any changes in luminescence. However, if certain fluorescent molecules were encapsulated, it was expected that the phase transition of PCN-526 would alter the distance and interaction between guest and host molecules in addition to guest and other guest molecules, therefore inducing changes in PL. In this work, we discovered a temperature-triggered reversible SC-SC transformation in PCN-526. A set of control experiments was performed to obtain detailed mechanistic aspects of the phase transition. In addition, we modulated and introduced responsive PL of PCN-526 by accommodating a series of luminescent guest molecules in the channel. This SC-SC transformation provides a unique strategy to establish a connection between structure and luminescence and indicates the structure change of the material by easily detectable physical properties.

EXPERIMENTAL SECTION

General Information. Commercial chemicals are used as purchased unless otherwise designated. Detailed chemical sources are provided in the Supporting Information (SI).

Instrumentation. Powder X-ray diffraction (PXRD) was carried out with a BRUKER D8-Focus Bragg–Brentano X-ray powder diffractometer equipped with a Cu sealed tube ($\lambda = 1.54178$) at 40 kV and 40 mA. About 10 mg of the sample was heated on a TGA Q500 thermogravimetric analyzer from room temperature to 1073 K at a ramp rate of 2 K/min under a N_2 flow of 15 mL min^{-1} . Nuclear magnetic resonance (NMR) data were collected on a Mercury 300 spectrometer. Inductively coupled plasma emission - mass spectrometry (Laser Ablation) was carried out by PerkinElmer DRCII ICP-MS with both solution and laser ablation capabilities. Energy dispersive X-ray spectroscopy (EDS) was carried out by Hitachi S-4800 equipped with X-ray mapping. PTI QuantaMaster series spectrofluorometer equipped with arc lamp provides illumination for steady-state measurements for both emission and excitation scans. A Xenon arc lamp provides pulsed illumination for measuring phosphorescence lifetimes. Additionally, some laser and LED sources are available at specific wavelengths that can be attached for collecting fluorescence lifetime measurements. PL studies at 77 K were acquired with NMR tube as sample holder in a cold finger dewar filled with liquid nitrogen. Felix32 software was used to collect and analyze excitation scans, emission scans, and lifetime measurements.

Synthesis of PCN-526. Solvothermal reaction of $CdCl_2 \cdot 2H_2O$ (30 mg) and 5,10,15,20-tetrakis[4-(2H-tetrazol-5-yl)phenyl]porphyrin (H_2TTPP , 8 mg) ligand in the mixture of N,N' -dimethylacetamide (DMA) (2.5 mL) and methanol (0.5 mL) at 413 K gave rise to dark-purple cuboid crystals of PCN-526. Yield: 67%.

Synthesis of PCN-527. Solvothermal reaction of $CdCl_2 \cdot 2H_2O$ (30 mg) and H_2TTPP (8 mg) in the mixture of DMF (2.5 mL) and methanol (0.9 mL) at 338 K gave rise to dark-purple cuboid crystals of PCN-527. Yield: 78%.

Synthesis of PCN-528. Solvothermal reaction of $MnCl_2 \cdot 2H_2O$ (30 mg) and H_2TTPP (8 mg) in the mixture of DMF (2.5 mL) and methanol (0.9 mL) at 338 K gave rise to dark-purple cuboid crystals of PCN-528. Yield: 52%.

Preparation of PCN-526^{110 K-BPDC}. As-synthesized samples PCN-526 (10 mg) were washed with fresh DMA and immersed in a solution of 20 mg biphenyl-4,4'-dicarboxylic acid (BPDC) in 3 mL DMA. The mixture was allowed to stand at room temperature for 12 h. A crystal was selected, and single-crystal X-ray diffraction data were collected at 110 K. The same procedure was followed to prepare the samples treated with benzene, toluene, benzoic acid, terephthaldehyde (TPA), 1,5-diamino-naphthalene (DAN), and BPDC.

Preparation of PCN-526^{110 K-Na}. As-synthesized samples PCN-526 (10 mg) were washed with fresh DMA and immersed in a solution of 20 mg $NaNO_3$ in 3 mL DMA. The mixture was allowed to stand at

room temperature for 12 h. A crystal was selected, and single-crystal X-ray diffraction data were collected at 110 K.

Preparation of guest@PCN-526 Samples for Luminescence Studies. Herein, the encapsulation of naphthalene in pristine PCN-526 is taken as an example to describe the preparation procedure of guest@PCN-526. In order to minimize the error caused by dilution and control the signal in measuring range, a solution of 5 mg naphthalene in 1 mL DMA was prepared and measured with UV–vis spectroscopy. As-synthesized pristine PCN-526 (83 mg) was soaked in the solution and agitated to ensure sufficient contact between the solid and solution phases at 298 K. The mixture was centrifuged, and the supernatant was collected for UV measurement every 10 min (Figure S4 in SI). The absorbance of the sorbed band was proportional to the concentration of naphthalene according to the Beer–Lambert law. Therefore, the loading amount can be calculated by measuring the concentration of supernatant and then subtracting from the initial solute (5 mg). The detailed information is listed in Table S4. After the guest molecules were encapsulated, the unit cell parameters of complexes were determined by single-crystal X-ray diffraction and are listed in Table 2.

Single X-ray Crystallography. Single-crystal X-ray data frames were collected using the program APEX 2 and processed using the program SAINT routine. The data were corrected for absorption and beam corrections based on the multiscan technique as implemented in SADABS. The structure was solved by direct methods and refined by full-matrix least-squares on F^2 with anisotropic displacement using the SHELXTL software package. Non-hydrogen atoms were refined with anisotropic displacement parameters during the final cycles. Hydrogen atoms on carbon and nitrogen were calculated in ideal positions with isotropic displacement parameters set to $1.2 \times U_{eq}$ of the attached atoms. Contributions to scattering due to these solvent molecules were removed using the SQUEEZE routine of PLATON, and the structures were then refined again using the data generated. Solvent molecules are not represented in the unit cell contents (chemical formula) in the crystal data. Details are given in SI. Crystallographic data and structural refinements for PCN-526^{298 K}, PCN-526^{110 K}, PCN-526^{110 K-BPDC}, PCN-526^{110 K-Na}, PCN-527, and PCN-528 are given in Table S1 (CCDC 1063029–1063034).

RESULTS AND DISCUSSION

Phase Transition. Single-crystal X-ray analysis at room temperature revealed that PCN-526 crystallizes in the tetragonal $P4/mmm$ space group (denoted by PCN-526^{298 K}). Chloride-centered square planar $[Cd_4Cl]^{7+}$ clusters are connected with eight TTPP ligands to form a 3D network with open channels of about 21 Å. The framework adopts a 4,8-connected *scu-a* topology with a point symbol of $\{4^4 \cdot 6^2\}_2 \{4^{16} \cdot 6^{12}\}$ by considering $[Cd_4Cl]^{7+}$ clusters as eight-connected nodes and TCPP ligands as four-connected nodes.^{8,9} The two uncoordinated N atoms of adjacent tetrazolate rings on different TTPP ligands bridge Cd(II) ions (occupancy is about 25%) along the edges of the square of the cluster. The partially occupied Cd(II) ions can be viewed as extra-framework metal sites, which were also observed in a 3,8-connected Mn-MOF.¹⁰ There is an isolated Cd(II) in the channel of the framework close to the $[Cd_4Cl]^{7+}$ node for charge balance. At room temperature, the free Cd(II) in the channels is highly delocalized, which cannot be assigned with a reasonable thermal parameter. However, the existence of isolated Cd(II) can be clearly confirmed by single-crystal X-ray diffraction collected at 110 K, as we will discuss subsequently in PCN-526^{110 K}. TTPP ligands in the framework adopt an ideal planar conformation with four tetrazol-phenyl moieties perpendicular to the porphyrin center (Figure 1). A five-coordinated Cd(II) ion occupies the porphyrin center adopting a square pyramidal geometry with chloride atom in the vertex position.

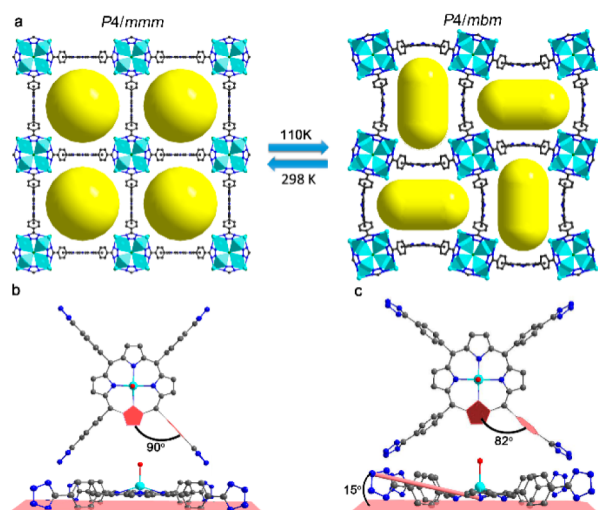


Figure 1. (a) Structures of PCN-526^{298 K} and PCN-526^{110 K} and (b) the ligand conformations in PCN-526^{298 K} and (c) in PCN-526^{110 K}.

Upon exposure to a liquid nitrogen flow at 110 K, PCN-526 underwent a SC-SC transformation from the *P4/mmm* to the *P4/mbm* space group (denoted by PCN-526^{110 K}). Single-crystal X-ray diffraction indicates that the framework still maintains the *scu-a* topology, but the [Cd₄Cl]⁷⁺ clusters display an apparent rotation along the *c* axis after structural transformation (Figure 1). Moreover, the four tetrazole-phenyl moieties deviate from the perpendicular positions of the porphyrin center with a dihedral angle of about 82° (Figure 1c). As a result, the TTPP ligand slightly deforms into a concave conformation accompanied by an obvious variation of the Cd(II)–N bonds in the porphyrin center (Table S2). The conformational change of the ligand induces the open channel of the framework to twist from square (21 × 21 Å without considering the van der Waals radius) to rectangular (23 × 14 Å), as shown in Figure 1a. We chose four different temperatures to determine the unit cell parameters of PCN-526 during the slow cooling down process (Table S3), and it is interesting to find that this SC-SC transformation was only achieved through an abrupt drop in temperature, such as with a cooling rate of >20 K/min, obtained by immediately placing a

crystal in the single-crystal X-ray diffractometer at 110 K or lower. Slow cooling did not induce the structural transformation. Moreover, the structure converted back to *P4/mmm* upon being warmed to 298 K, indicating a reversible SC-SC transformation. Usually, the unit cell reduces with the decrease of temperature for the positive thermal expansion materials, and it is the same for PCN-526 by slowly decreasing the temperature. Although quenching treatment is very rarely applied in the MOF field, it is widely utilized in material science to forbid or force a material to undergo a phase transition.^{11a} The distinct behaviors of PCN-526 by different heat treatments of quenching and slowly cooling down attracted our interest in investigating the structural characteristic accounting for the phase transition.

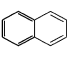
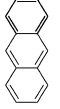
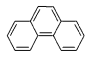
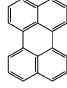
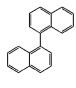
Mechanistic Studies. Structural roles were first examined to gain insight into the mechanism of the phase transition. Since the Cd(II) ion in the porphyrin center of the TTPP ligand underwent evident conformational changes during the process, we first speculated that the presence of such Cd(II) ions may be crucial for the structural transformation. Therefore, we attempted to synthesize an isostructural MOF of PCN-526 without metal species chelated in porphyrin center, denoted by PCN-527. The low reaction temperature makes the deprotonation of the porphyrin center difficult, and hence there was no Cd ion chelated. It turned out that PCN-527 displayed the same SC-SC transformation as PCN-526 (Table 1). This control experiment rules out a decisive role of Cd(II) behind the transformation despite its apparent conformational change as a result of the transformation. It is known that phase transitions are usually related to stress or strain changes in materials.¹¹ With this consideration in mind, we treated PCN-526 with certain molecules which can provide strong interactions with the framework. Six molecules, benzene, toluene, benzoic acid, TPA, DAN, and BPDC, were selected based on functional groups and molecular size (Table 1). After treatment with DMA solutions containing these molecules, the unit cell parameters of PCN-526 were characterized by single-crystal X-ray diffraction. The results indicate that phase transitions of PCN-526 were forbidden when treated with benzoic acid, TPA, DAN and BPDC, likely due to interactions with the framework through the terminal groups of the encapsulated molecules. In contrast, phase transitions were

Table 1. Unit Cell Parameters of PCN-526, PCN-527^{110 K}, and PCN-526 at 110 K after Treating with Different Molecules

	PCN-526 ^{298K}	PCN-526 ^{110K}	PCN-527 ^{110K}	PCN-528 ^{110K}	NaNO ₃	Ben-zene	Tolu-ene	Benzo-ic acid	TPA	DAN	BPDC
Phase transition	Allowed	Allowed	Forbidden	Forbidden	Forbidden	Allowed	Allowed	Forbidden	Forbidden	Forbidden	Forbidden
<i>a</i> , <i>b</i> (Å)	21.60	27.85	27.81	20.55	20.33	28.30	28.18	20.30	19.61	19.97	19.96
<i>c</i> (Å)	19.38	20.45	20.60	19.91	20.29	20.18	20.34	20.20	19.59	20.33	20.47
α , β , γ (°)	90	90	90	90	90	90	90	90	90	90	90
<i>V</i> (Å ³)	9043	15862	15930	8406	8391	16160	16154	8326	7537	8108	8156

allowed after the treatment using molecules hypothesized to interact with the framework more weakly, such as benzene or toluene. This phenomenon was further confirmed when the polycyclicaromatic compounds were encapsulated for PL studies as discussed in the following section (Table 2).

Table 2. Unit Cell Parameters of PCN-526 after Incorporating Different Fluorescent Molecules

					
	Naphth -alene	Anthra -cene	Phenan -threne	Pery -lene	1,1'- Binaphthyl
Phase transition	Allowed	Allowed	Allowed	Allowed	Allowed
a, b (Å)	28.72	28.39	28.76	28.36	28.25
c (Å)	20.21	20.42	20.32	20.49	19.69
α, β, γ (°)	90	90	90	90	90
V(Å ³)	16674	16460	16803	16481	15717

As a representative, single-crystal X-ray diffraction data of PCN-526^{110 K} after treatment with BPDC solution (denoted by PCN-526^{110 K-BPDC}) were collected, and the structure was solved and refined (Figure 2). The result indicates that PCN-

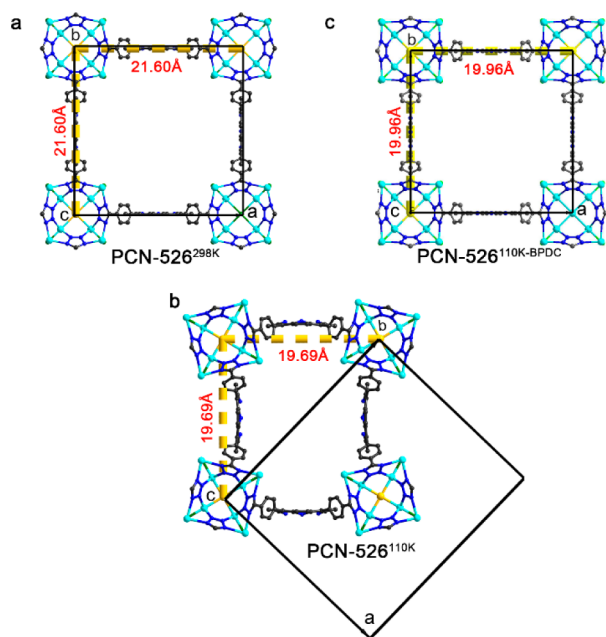


Figure 2. Structures of (a) PCN-526^{298 K}, (b) PCN-526^{110 K}, and (c) PCN-526^{110 K-BPDC}.

526^{110 K-BPDC} has the same structure as PCN-526^{298 K} but with a remarkably shorter [Cd₄Cl]⁷⁺ distance of 19.96 Å compared with 21.60 Å in PCN-526^{298 K} (based on the center to center Cl–Cl distance). Further analysis of the structure of PCN-526^{110 K-BPDC} indicates that the [Cd₄Cl]⁷⁺ clusters display an apparent rotation along the *c* axis after structural transformation while retaining the square arrangement (as highlighted by the yellow dotted lines in Figure 2c). Moreover, it is interesting to

find that the cluster distance in PCN-526^{110 K-BPDC} is close to that of PCN-526^{110 K}, as well as those samples treated with solutions of benzoic acid, TPA, and DAN, in which the transformation was forbidden (Cl–Cl distances equal to the *a* and *b* axes lengths which are listed in Table 1). Usually, it is observed that the unit cell size decreases after temperature reduction.¹² The difference for PCN-526 is that the porphyrin ligand distorts from planarity during shrinkage of the unit cell, resulting in the phase transition. However, after treatment with BPDC as well as the above-mentioned solutions, PCN-526 shrunk into a smaller volume without deforming the conformation of the ligands. Although we cannot determine the specific position of BPDC in framework by single X-ray diffraction because of the low density, a very interesting variation was observed in the refined structure: the partially occupied Cd(II) ion in the extra-framework metal sites has a much lower occupancy compared with that in the pristine PCN-526 (Figure 3a,b). The change of occupancy is probably

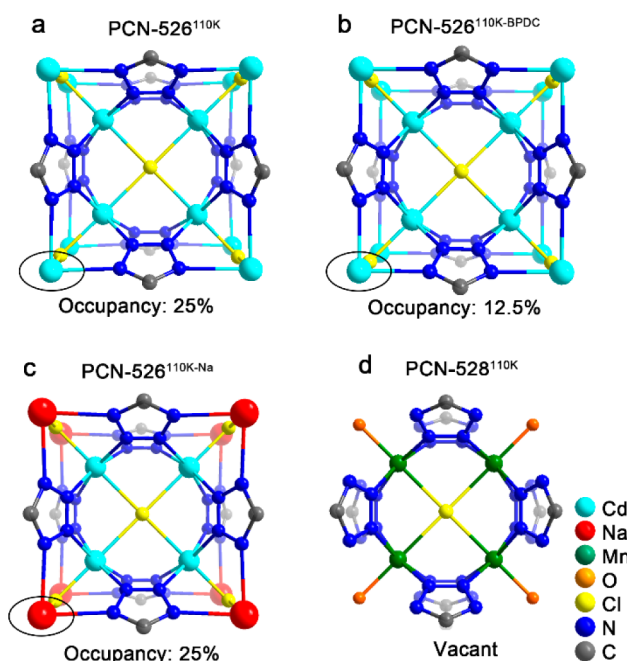


Figure 3. Representative of the [Cd₄Cl]⁷⁺ cluster and extra-framework sites (highlighted with black circle) (a) in PCN-526^{110 K}, (b) in PCN-526^{110 K-BPDC}, (c) in PCN-526^{110 K-Na}, and (d) the [Mn₄Cl]⁷⁺ cluster with vacant extra-framework sites in PCN-528^{110 K}.

due to the influence of BPDC molecules which can competitively bond with Cd ions in the extra-framework sites. This discovery implies that the partially occupied Cd(II) may be a very important structural cause for the transformation, and we were inspired to investigate further by continuing to alter the composition of the metal cluster.

The as-synthesized PCN-526 was immersed in NaNO₃ solution for 12 h. Single-crystal X-ray diffraction reveals that the Cd(II) ions in the extra-framework sites were substituted by Na ions with an occupancy of about 25% (Figure 3c), and this result is consistent with the ICP analysis (Cd: Na = 4:1, Section 8 in SI). Most significantly, PCN-526 failed to undergo SC-SC transformation after the treatment (denoted by PCN-526^{110 K-Na}, as shown in Table 1). This observation indicates that the substitution of Cd ions with the relatively light metal Na ions forbids the phase transition during the temperature

decrease. Therefore, we speculate that the analogous structure of PCN-526 without partially occupied metals, if it exists, should not have the same phase transition behavior. Reaction of MnCl_2 and TPPP ligand produced PCN-528 which crystallizes in the same space group as PCN-526 but without partially occupied metal ions in the extra-framework sites (Figure 3d).¹³ As expected, PCN-528 did not display the structure transformation by changing the temperature, indicating the partially occupied Cd(II) ions in the exterior of metal cluster play a decisive role for the structural transformation.

Based on the thermodynamic principle, the phase transition is a consequence of a compromise: the energy tends to make the material ordered and the entropy associated with the temperature tends to disobey the current order.^{11f-h} In PCN-526, the disordered distribution of Cd(II) ions in the extra-framework sites implies that the orientation of Cd(II) differ randomly in every unit cell. Usually, the observed disordered atoms can be viewed as real movement in crystal.¹¹ⁱ Therefore, it is reasonable to infer that the random movement of Cd(II) ions may induce anisotropic stress or strain at the instant of abrupt drop in temperature and hence increase the tendency of breaking the original order of material to trigger the phase transition.¹⁴ However, such tendency was diminished when the framework was treated with some molecules which can interact with the partially occupied metal ions, producing less uneven force toward framework upon abrupt drop in temperature. Therefore, the structural transformation was effectively forbidden by lowering the occupancy of disordered metal (PCN-526^{110 K-BPDC}) or substitution of the heavy metal ions with light metal ions like in PCN-526^{110 K-Na}. This observation was further supported by the investigation on PCN-528, an analogous structure with vacancies in the extra-framework sites, which cannot display the same SC-SC structure transformation that PCN-526 does. Actually, very similar phenomena were observed in some ammonium salts where the reorientation or the ordered–disordered processes of anions has been proven to account for the phase transition.^{11j,k}

Potential Applications. We sought to explore the quenching-triggered phase transition for potential applications as sensors or indicators by taking advantage of the changes in structure. The porous framework can act as an efficient scaffold that noncovalently traps guest molecules for variety of applications.¹⁵ With guest molecules incorporated, phase transitions involving an alteration in channel size would provide a unique pathway to change host–guest interactions and achieve efficient energy transfers. Thus, five polycyclic aromatic molecules, including naphthalene, phenanthrene, anthracene, perylene, and 1,1'-binaphthyl, with gradually increasing size across the series, were encapsulated in PCN-526, and the effect on PL properties was investigated.

The successful encapsulation of luminescent molecules in frameworks was confirmed by UV–vis absorption spectra (Section 6 in SI). The phase transitions after guest incorporation were then confirmed by single-crystal X-ray diffraction (Table 2). The emission wavelength of PCN-526 displays an intense and broad emission peak with a maximum at 407 nm upon excitation at 323 nm, and the SC-SC transformation does not result any changes in luminescence (Figures S7 and S8). When naphthalene molecules are loaded, the emission of naphthalene@PCN-526 displays almost exactly the same spectrum as that of PCN-526 (Figure 4a). Incorporation of phenanthrene in the framework results in a slight red shift of the emission compared with PCN-526

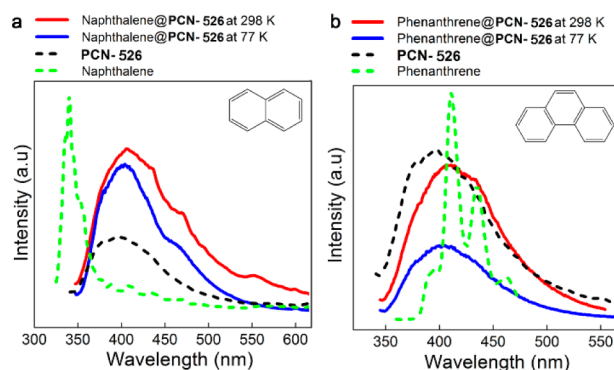


Figure 4. Emission spectra of (a) naphthalene and (b) phenanthrene@PCN-526 at 298 K (red) and 77 K (blue), respectively, PCN-526 (black), and free molecules (green).

(Figure 4b). These results indicate that there is no energy transfer between the guest molecules and the host matrix. In order to achieve efficient energy transfer, we explored possible routes of fluorescence resonance energy transfer (FRET) from organic linker to encapsulated guest acceptor.

FRET describes the transfer of excited-state energy from an initially excited donor to an acceptor. The efficiency of energy transfer in FRET is very sensitive to the distance between the relative orientation of the donor and the acceptor's dipole moments.^{15a,b} This process would occur if the emission spectrum of the donor overlaps with the adsorption spectrum of the acceptor. Anthracene was selected because its excitation spectrum overlaps very well with the emission spectrum of PCN-526 (Figure 5a). When anthracene@PCN-526 is excited

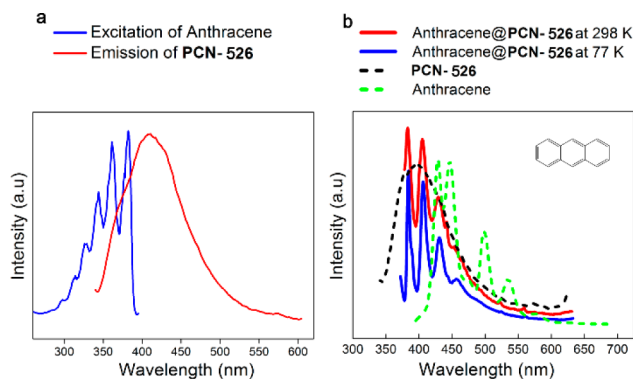


Figure 5. The emission spectrum of (a) PCN-526 and excitation of anthracene and (b) anthracene@PCN-526 at 298 K (red) and 77 K (blue), respectively, PCN-526 (black), and free molecules (green).

at 335 nm, the emission of PCN-526 is completely quenched, whereas a strong anthracene emission appears with an approximate 60 nm blue shift as shown in Figure 5b, indicating an efficient light harvesting process. This resonance energy transfer is further supported by the excitation spectrum of anthracene@PCN-526 collected at the anthracene emission (410 nm), in which a maximum peak at 335 nm clearly suggests the contribution of PCN-526 to the observed emission (Figure S11). In addition, the fluorescence decay profile of the anthracene@PCN-526 monitored at 407 nm shows a longer lifetime of 3.19 ns upon excitation at 395 nm (the anthracene excitation) compared to a lifetime of 0.44 ns upon excitation at 340 nm (the pristine PCN-526 excitation), providing further proof for energy transfer (Figures S12 and S13).

Naphthalene@PCN-526, phenanthrene@PCN-526, and anthracene@PCN-526 display the same emission band at 298 and 77 K. These findings indicate that the shrinkage of the channel, caused by a structural transformation, does not change the host–guest interaction and the interaction between guest molecules. However, when a larger guest molecule, perylene, was encapsulated, the complex displayed new emission bands at higher wavelength (Figure 6a). The phenyl rings in perylene

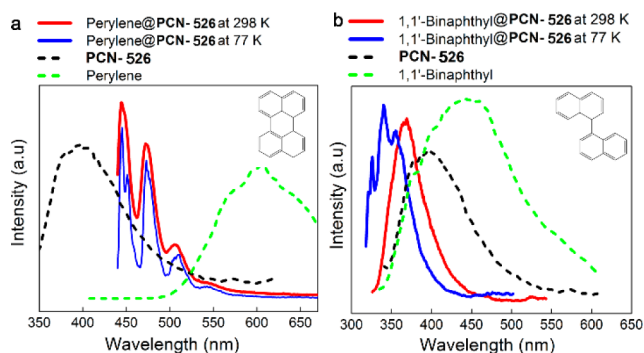


Figure 6. Emission spectra of (a) perylene and (b) 1,1'-binaphthyl @ PCN-526 at 298 K (red) and 77 K (blue), respectively, PCN-526 (black), and free molecules (green).

may be parallel with the porphyrin center, promoting the π – π^* interaction, thus facilitating the host–guest energy transfer.¹⁶ Moreover, the emission of perylene@PCN-526 displays an obvious peak splitting at 77 K compared with 298 K. A peak split is usually caused by temperature, stress, pressure, and/or energy transfer between two particles.¹⁷ A plausible explanation is that the distances or orientations between the host and guest or the interguest molecules are changed due to the structural transformation. To validate this hypothesis, we encapsulated 1,1'-binaphthyl to investigate the PL of the complex at 298 and 77 K. The single bond of 1,1'-binaphthyl would allow the two naphthalene moieties to change relative orientations freely from external stimuli. As expected, the emission of 1,1'-binaphthyl@PCN-526 displayed a more evident peak splitting with a 30 nm blue-shift at 77 K compared with the emission at 298 K as shown in Figure 6b. Moreover, the blue shift is also considered to have been caused by the alteration of the aggregated structure.¹⁸ These results confirm the occurrence of a temperature triggered structure transformation, and more interestingly, the transformation can be responsively expressed by another readily detectable physical property: an evident difference in luminescence phenomena at 298 and 77 K.

The systematic PL investigations of different guest@PCN-526 complexes indicate that the PL of complexes is greatly affected by the size of polycyclic aromatic molecules. Incorporation of molecules with relatively small size, such as naphthalene and phenanthrene, has a negligible impact on the emission band of host matrices. However, when the guest molecules with larger size, such as perylene and 1,1'-binaphthyl, were incorporated, the host–guest interaction and the interaction between guest molecules influences the energy transfer pathways and results in the appearance of guest emissions or a new emission band. By exploring the FRET mechanism, PCN-526 acts as an efficient light harvesting scaffold for anthracene guest molecules. PL of the pristine PCN-526 initially was unchanged by the SC-SC transformation. However, with suitable guest molecules entrapped

inside the pore, the luminescence of guest@PCN-526 displays a blue shift and apparent peak splitting in response to the structural transformation and host–guest interactions. In this way, we have demonstrated a novel method to reveal normally imperceptible structural information by readily detectable PL phenomena.

CONCLUSION

In this study, we have discovered a reversible crystallinity-preserving phase transition in PCN-526 triggered by an abrupt change in temperature. Remarkably, we are able to observe the phase transition allowed and forbidden behaviors which elucidate the structural causes for the transformation and provide mechanistic insight into the phase transition. Moreover, we have demonstrated that the unique phase transition properties can be utilized as a platform to responsively indicate the structural change of materials by luminescence, which might provide a new perspective for design of smart materials, such as sensing device and logic gates.

ASSOCIATED CONTENT

Supporting Information

CCDC 1063029–1063034 contains the supplementary crystallographic data for MOFs discussed in this report. These data can be obtained from The Cambridge Crystallographic Data Centre via www.ccdc.cam.ac.uk/data_request/cif. Full details for materials, ligand synthesis, synthesis of samples, X-ray crystallography, thermal stability analysis, encapsulation of guest molecules in sample, PL studies, ICP and EDS results. The Supporting Information is available free of charge on the ACS Publications website at DOI: 10.1021/jacs.5b02999.

AUTHOR INFORMATION

Corresponding Author

*zhou@chem.tamu.edu

Author Contributions

§These authors contributed equally.

Notes

The authors declare no competing financial interest.

ACKNOWLEDGMENTS

The PL studies of this research was supported by the Center for Gas Separations Relevant to Clean Energy Technologies, an Energy Frontier Research Center funded by the U.S. Department of Energy, Office of Science, Office of Basic Energy Sciences under award no. DE-SC0001015. It was funded in part by the Advanced Research Projects Agency – Energy (ARPA-E), U.S. Department of Energy, under award no. DE-AR0000249. We gratefully acknowledge the Robert A. Welch Foundation (A-1725) and the Office of Naval Research (N00014-14-1-0720) for support of the structural analyses of this work. D.L. and C.Z. thank the supports of Natural Science Foundation of China (nos. 21136001 and 21276008) and National Key Basic Research Program of China (“973”) (2013CB733503). D.L. also thanks the support of China Scholarship Council (CSC, no. 201208110375).

REFERENCES

- (1) (a) Zhou, H.-C.; Long, J. R.; Yaghi, O. M. *Chem. Rev.* **2012**, *112*, 673–674. (b) Zhou, H.-C.; Kitagawa, S. *Chem. Soc. Rev.* **2014**, *43*, 5415–5418.

- (2) (a) Suh, M. P.; Ko, J. W.; Choi, H. J. *J. Am. Chem. Soc.* **2002**, *124*, 10976–10977. (b) Serre, C.; Millange, F.; Thouvenot, C.; Noguès, M.; Marsolier, G.; Louër, D.; Férey, G. *J. Am. Chem. Soc.* **2002**, *124*, 13519–13526. (c) Maji, T. K.; Mostafa, G.; Matsuda, R.; Kitagawa, S. *J. Am. Chem. Soc.* **2005**, *127*, 17152–17153. (d) Serre, C.; Mellot-Draznieks, C.; Surlé, S.; Audebrand, N.; Filinchuk, Y.; Férey, G. *Science* **2007**, *315*, 1828–1831. (e) Inumaru, K.; Kikudome, T.; Fukuoka, H.; Yamanaka, S. *J. Am. Chem. Soc.* **2008**, *130*, 10038–10039. (f) Maji, T. K.; Matsuda, R.; Kitagawa, S. *Nat. Mater.* **2007**, *6*, 142–148. (g) Das, S.; Kim, H.; Kim, K. *J. Am. Chem. Soc.* **2009**, *131*, 3814–3815. (h) Plabst, M.; McCusker, L. B.; Bein, T. *J. Am. Chem. Soc.* **2009**, *131*, 18112–18118. (i) Lee, J. Y.; Lee, S. Y.; Sim, W.; Park, K.-M.; Kim, J.; Lee, S. S. *J. Am. Chem. Soc.* **2008**, *130*, 6902–6903. (j) Demadis, K. D.; Papadaki, M.; Aranda, M. A. G.; Cabeza, A.; Olivera-Pastor, P.; Sanakis, Y. *Cryst. Growth Des.* **2010**, *10*, 357–364.
- (3) (a) Horike, S.; Shimomura, S.; Kitagawa, S. *Nat. Chem.* **2009**, *1*, 695–704. (b) Zeng, M.-H.; Feng, X.-L.; Zhang, W.-X.; Chen, X.-M. *Dalton Trans.* **2006**, 5294–5303. (c) Liu, D.; Liu, X.; Liu, Y.; Yu, Y.; Chen, F.; Wang, C. *Dalton Trans.* **2014**, *43*, 15237–15244.
- (4) (a) Martí-Rujas, J.; Islam, N.; Hashizume, D.; Izumi, F.; Fujita, M.; Kawano, M. *J. Am. Chem. Soc.* **2011**, *133*, 5853–5860. (b) Tian, J.; Saraf, L. V.; Schwenzer, B.; Taylor, S. M.; Brechin, E. K.; Liu, J.; Dalgarno, S. J.; Thallapally, P. K. *J. Am. Chem. Soc.* **2012**, *134*, 9581–9584. (c) Toh, N. L.; Nagarathinam, M.; Vittal, J. J. *Angew. Chem., Int. Ed.* **2005**, *44*, 2237–2241. (d) Nagarathinam, M.; Vittal, J. J. *Angew. Chem., Int. Ed.* **2006**, *45*, 4337–4341. (e) Liu, D.; Ren, Z.-G.; Li, H.-X.; Lang, J.-P.; Li, N.-Y.; Abrahams, B. F. *Angew. Chem., Int. Ed.* **2010**, *49*, 4767–4770.
- (5) Mir, M. H.; Koh, L. L.; Tan, G. K.; Vittal, J. J. *Angew. Chem., Int. Ed.* **2010**, *49*, 390–393.
- (6) (a) Hauptvogel, I. M.; Biedermann, R.; Klein, N.; Senkowska, I.; Cadiau, A.; Wallacher, D.; Feyerherm, R.; Kaskel, S. *Inorg. Chem.* **2011**, *50*, 8367–8374. (b) Zhang, L.-G.; Gu, W.; Dong, Z.; Liu, X.; Li, B. *CrystEngComm* **2008**, *10*, 1318–1320. (c) López-Beceiro, J.; Gracia-Fernández, C.; Gómez-Barreiro, S.; Castro-García, S.; Sánchez-Andújar, M.; Artiaga, R. *J. Phys. Chem. C* **2012**, *116*, 1219–1224. (d) Bernini, M. C.; Gándara, F.; Iglesias, M.; Snejko, N.; Gutiérrez-Puebla, E.; Brusau, E. V.; Narda, G. E.; Monge, M. Á. *Chem.—Eur. J.* **2009**, *15*, 4896–4905. (e) Spencer, E. C.; Kiran, M. S. R. N.; Li, W.; Ramamurty, U.; Ross, N. L.; Cheetham, A. K. *Angew. Chem., Int. Ed.* **2014**, *53*, 5583–5586.
- (7) (a) Committee on New Sensor Technologies: Materials and Applications, Commission on Engineering and Technical Systems. National Research Council. *Expanding the Vision of Sensor Materials*; The National Academies Press: Washington, DC, 1995. (b) Kloxin, A. M.; Kloxin, C. J.; Bowman, C. N.; Anseth, K. S. *Adv. Mater.* **2010**, *22*, 3484–3494. (c) Jiang, H.-L.; Feng, D.; Wang, K.; Gu, Z.-Y.; Wei, Z.; Chen, Y.-P.; Zhou, H.-C. *J. Am. Chem. Soc.* **2013**, *135*, 13934–13938.
- (8) Delgado-Friedrichs, O.; O’Keeffe, M.; Yaghi, O. M. *Acta Crystallogr.* **2006**, *A62*, 350–355.
- (9) (a) Wu, J.-Y.; Yang, S.-L.; Luo, T.-T.; Liu, Y.-H.; Cheng, Y.-W.; Chen, Y.-F.; Wen, Y.-S.; Lin, L.-G.; Lu, K.-L. *Chem.—Eur. J.* **2008**, *14*, 7136–7139. (b) Ma, L.; Mihalcik, D. J.; Lin, W. *J. Am. Chem. Soc.* **2009**, *131*, 4610–4612. (c) Cheng, X.; Duan, X.-Y.; Liu, T.; Wang, F.-M.; Lu, C.-S.; Meng, Q.-J. *Inorg. Chem. Commun.* **2010**, *13*, 818–821. (d) Tan, C.; Yang, S.; Champness, N. R.; Lin, X.; Blake, A. J.; Lewis, W.; Schröder, M. *Chem. Commun.* **2011**, *47*, 4487–4489. (e) Mihalcik, D. J.; Zhang, T.; Ma, L.; Lin, W. *Inorg. Chem.* **2012**, *51*, 2503–2508. (f) Xue, Y.-S.; He, Y.; Ren, S.-B.; Yue, Y.; Zhou, L.; Li, Y.-Z.; Du, H.-B.; You, X.-Z.; Chen, B. *J. Mater. Chem.* **2012**, *22*, 10195–10199. (g) Lin, Z.-J.; Huang, Y.-B.; Liu, T.-F.; Li, X.-Y.; Cao, R. *Inorg. Chem.* **2013**, *52*, 3127–3132.
- (10) Dincă, M.; Dailly, A.; Liu, Y.; Brown, C. M.; Neumann, D. A.; Long, J. R. *J. Am. Chem. Soc.* **2006**, *128*, 16876–16883.
- (11) (a) Papon, P.; Leblond, J.; Meijer, P. H. E. *The Physics of Phase Transitions: Concepts and Applications*; Springer-Verlag: Berlin Heidelberg, 2006. (b) Bahr, D. F.; Reid, J. A.; Mook, W. M.; Bauer, C. A.; Stumpf, R.; Skulan, A. J.; Moody, N. R.; Simmons, B. A.; Shindel, M. M.; Allendorf, M. D. *Phys. Rev. B* **2008**, *77*, 059902.
- (c) Neimark, A. V.; Coudert, F.-X.; Boutin, A.; Fuchs, A. H. *J. Phys. Chem. Lett.* **2010**, *1*, 445–449. (d) Tan, J. C.; Cheetham, A. K. *Chem. Soc. Rev.* **2011**, *40*, 1059–1080. (e) Boutin, A.; Coudert, F.-X.; Springuel-Huet, M.-A.; Neimark, A. V.; Férey, G.; Fuchs, A. H. *J. Phys. Chem. C* **2010**, *114*, 22237–22244. (f) Reynaud, F. *Phys. Stat. Sol.(a)* **1982**, *72*, 11–59. (g) Rao, C. N. R.; Rao, K. J. *Phase Transitions in Solids: An Approach to the Study of the Chemistry and Physics of Solids*; McGraw-Hill: New York, 1978. (h) Buerger, M. J. *Phase Transitions in Solids*; John Wiley: New York, 1951. (i) Müller, P.; Herbst-Irmer, R.; Spek, A.; Schneider, T.; Sawaya, M. *Crystal Structure Refinement: A Crystallographer’s Guide to SHELXL*; Oxford University Press: Oxford, U.K., 2006. (j) Migdal-Mikuli, A.; Liszka-Skoczylas, M.; Mikuli, E. *Phase Transit.* **2007**, *80*, 547–557. (k) Janik, J. M.; Janik, J. A.; Migdal-Mikuli, A.; Mikuli, E.; Otnes, K. *Physica B* **1991**, *168*, 45–52.
- (12) (a) Krishnan, R. S.; Srinivasan, R.; Devanarayanan, S. *Thermal Expansion of Crystals*; Pergamon Press: Oxford, U.K., 1979. (b) DeVries, L. D.; Barron, P. M.; Hurley, E. P.; Hu, C.; Choe, W. *J. Am. Chem. Soc.* **2011**, *133*, 14848–14851. (c) Wang, X.-F.; Wang, Y.; Zhang, Y.-B.; Xue, W.; Zhang, J.-P.; Chen, X.-M. *Chem. Commun.* **2012**, *48*, 133–135.
- (13) Guo, Z.; Yan, D.; Wang, H.; Tesfagaber, D.; Li, X.; Chen, Y.; Huang, W.; Chen, B. *Inorg. Chem.* **2015**, *54*, 200–204. In this work, the authors reported a manganese MOF, UTSA-57, with moderately high performance for C₂H₂/CH₄ separation. PCN-528 has the same structure with UTSA-57, while PCN-526 and PCN-527 are isorecticular with UTSA-57.
- (14) (a) Durandurdu, M. *Phys. Rev. B* **2009**, *80*, 024102. (b) Durandurdu, M. *Phys. Rev. B* **2010**, *81*, 174107. (c) Wakabayashi, Y.; Bizen, D.; Nakao, H.; Murakami, Y.; Nakamura, M.; Ogimoto, Y.; Miyano, K.; Sawa, H. *Phys. Rev. Lett.* **2006**, *96*, 017202.
- (15) (a) Hildebrandt, N.; Wegner, K. D.; Algar, W. R. *Coord. Chem. Rev.* **2014**, *273–274*, 125–138. (b) Suresh, V. M.; George, S. J.; Maji, T. K. *Adv. Funct. Mater.* **2013**, *23*, 5585–5590. (c) Lu, G.; Li, S.; Guo, Z.; Farha, O. K.; Hauser, B. G.; Qi, X.; Wang, Y.; Wang, X.; Han, S.; Liu, X.; DuChene, J. S.; Zhang, H.; Zhang, Q.; Chen, X.; Ma, J.; Loo, S. C. J.; Wei, W. D.; Yang, Y.; Hupp, J. T.; Huo, F. *Nat. Chem.* **2012**, *4*, 310–316. (d) Ibarra, I. A.; Hesterberg, T. W.; Chang, J.-S.; Yoon, J. W.; Holliday, B. J.; Humphrey, S. M. *Chem. Commun.* **2013**, *49*, 7156–7158. (e) Takashima, Y.; Martínez, V. M.; Furukawa, S.; Kondo, M.; Shimomura, S.; Uehara, H.; Nakahama, M.; Sugimoto, K.; Kitagawa, S. *Nat. Commun.* **2011**, *2*, 168. (f) Zheng, X.-L.; Liu, Y.; Pan, M.; Lü, X.-Q.; Zhang, J.-Y.; Zhao, C.-Y.; Tong, Y.-X.; Su, C.-Y. *Angew. Chem., Int. Ed.* **2007**, *46*, 7399–7403. (g) Li, Y.-A.; Ren, S.-K.; Liu, Q.-K.; Ma, J.-P.; Chen, X.; Zhu, H.; Dong, Y.-B. *Inorg. Chem.* **2012**, *51*, 9629–9635. (h) Lu, H.-S.; Bai, L.; Xiong, W.-W.; Li, P.; Ding, J.; Zhang, G.; Wu, T.; Zhao, Y.; Lee, J.-M.; Yang, Y.; Geng, B.; Zhang, Q. *Inorg. Chem.* **2014**, *53*, 8529–8537. (i) Colodrero, R. M. P.; Papanthanasios, K. E.; Stavgiannoudaki, N.; Olivera-Pastor, P.; Losilla, E. R.; Aranda, M. A. G.; León-Reina, L.; Sanz, J.; Sobrados, I.; Choquesillo-Lazarte, D.; García-Ruiz, J. M.; Atienzar, P.; Rey, F.; Demadis, K. D.; Cabeza, A. *Chem. Mater.* **2012**, *24*, 3780–3792.
- (16) Zhang, M.; Feng, G.; Song, Z.; Zhou, Y.-P.; Chao, H.-Y.; Yuan, D.; Tan, T. T. Y.; Guo, Z.; Hu, Z.; Tang, B. Z.; Liu, B.; Zhao, D. *J. Am. Chem. Soc.* **2014**, *136*, 7241–7244.
- (17) (a) Lee, S. J.; Kim, C. S.; Noh, S. K.; Chung, K. S.; Lee, K.-S. *J. Korean Phys. Soc.* **2007**, *51*, 1050–1054. (b) Olivero, P.; Bosia, F.; Fairchild, B. A.; Gibson, B. C.; Greentree, A. D.; Spizzirri, P.; Praver, S. *New J. Phys.* **2013**, *15*, 043027. (c) Choi, C. L.; Koski, K. J.; Sivasankar, S.; Alivisatos, A. P. *Nano Lett.* **2009**, *9*, 3544–3549. (d) Grant, C. D.; Crowhurst, J. C.; Hamel, S.; Williamson, A. J.; Zaitseva, N. *Small* **2008**, *4*, 788–794. (e) Sauer, M.; Hofkens, J.; Enderlein, J. *Handbook of Fluorescence Spectroscopy and Imaging: From Single Molecules to Ensembles*; Wiley-VCH Verlag GmbH & Co. KGaA: Weinheim, Germany, 2011.
- (18) (a) Kasha, M.; Rawls, H. R.; El-Bayoumi, M. A. *Pure Appl. Chem.* **1965**, *11*, 371–392. (b) Yanai, N.; Kitayama, K.; Hijikata, Y.; Sato, H.; Matsuda, R.; Kubota, Y.; Takata, M.; Mizuno, M.; Uemura, T.; Kitagawa, S. *Nat. Mater.* **2011**, *10*, 787–793.